Received: 12 April 2022 | Revised: 31 May 2022 | Accepted: 7 June 2022

DOI: 10.1111/ter.12610

RESEARCH ARTICLE

Terra Nova WILEY

A persistent Hadean–Eoarchean protocrust in the western Yilgarn Craton, Western Australia

Maximilian Dröllner | Christopher L. Kirkland | Milo Barham | Noreen J. Evans | Bradley J. McDonald

Timescales of Mineral Systems Group, School of Earth and Planetary Sciences, John de Laeter Centre, Curtin University, Perth, Western Australia, Australia

Correspondence
Maximilian Dröllner, Timescales of Mineral Systems Group, School of Earth and Planetary Sciences, John de Laeter Centre, Curtin University, Perth, WA, Australia.
Email: maximilian.droellner@postgrad.curtin.edu.au

Funding information
Minerals Research Institute of Western Australia, Grant/Award Number: M551; LIEF, Grant/Award Number: LE150100013

Abstract

Deciphering the composition and extent of Earth's earliest continents is hampered by the scarcity of preserved Hadean–Eoarchean material. Here, we report U–Pb and Lu–Hf data of detrital zircon from sediments proximal to the Archean Yilgarn Craton in Western Australia. This detrital cargo, in part derived from the crystalline basement of the southwestern Yilgarn Craton and its conjugate terranes, helps to resolve the ancient substrate of the craton. Zircon Hf isotopes point to a Hadean–Eoarchean crustal vestige that has remained isotopically coherent over 2 Gyr of episodic crustal reworking. Geophysical characteristics suggest a distinct 100,000 km^2 region of ancient protocrust beneath much of the western Yilgarn Craton, cropping out in the Narryer Terrane. Comparison with global data reveals similar Hf isotope trends in many other cratons documenting the widespread existence of voluminous protocrust and implying extensive reservoir extraction at *c.* 4,000–3,800 Ma.

1 | INTRODUCTION

The scarcity of well-preserved primary Hadean–Eoarchean material (e.g. Goodwin, 1996) impedes understanding of Earth's earliest continental crust. However, the geochemical legacy of ancient (>3,800 Ma) crustal seeds may survive reworking, conveying information on early crust–mantle differentiation into younger continental crust and ultimately the detrital record (Griffin, Belousova, Shee, Pearson, & O'Reilly, 2004; Guitreau et al., 2019). The Archean Yilgarn Craton (YC) in Western Australia (Figure 1a) has enabled significant advances in the understanding of the spatial and temporal development of early Earth's crust (e.g. Cassidy et al., 2006). The Narryer Terrane, in the northwestern YC, preserves some of the oldest continental crust on the planet (>3,700 Ma; Kinny, Williams, Froude, Ireland, & Compston, 1988) and hosts Earth's oldest terrestrial minerals (>4,400 Ma; Wilde, Valley, Peck, & Graham, 2001). Detritus in metasediments across the YC, granite chemistry and isotope geochemistry (e.g. Sm–Nd, Lu–Hf; Figure 1b,c) all hint at extensive cryptic components of an ancient protocrust of Hadean–Eoarchean age extending beyond the exposed Narryer Terrane (Morris & Kirkland, 2014; Petersson, Kemp, & Whitehouse, 2019; Wyche, Nelson, & Riganti, 2004). Detrital minerals are an important archive to decipher the evolution of our planet from the otherwise fragmentary ancient crustal record (e.g. Griffin et al., 2004). In this study, we perform U–Pb and Lu–Hf isotope measurements of detrital zircon to elucidate the post-Archean fate of early crust and its importance for crustal growth.

2 | GEOLOGICAL SETTING

The YC is dominated by characteristic Archean granite-greenstone crust and experienced major crustal growth at *c.* 2,750–2,600 Ma (Cassidy et al., 2006). The Albany-Fraser Orogen (AFO) is autochthonous to, and represents the dominantly Proterozoic hyperextension of, the southern and eastern margin of the YC (Figure 1a). Major tectonomagmatic events of the AFO took place at *c.* 1,710–1,650 Ma, 1,345–1,260 Ma and 1,215–1,140 Ma (Kirkland et al., 2011; Spaggiari, Kirkland, Smithies, Wingate, & Belousova, 2015). The 1,215–1,140 Ma event in the AFO was coeval with magmatism in the western Musgrave Province in central Australia (Figure 1a), despite being rooted on different basement (Kirkland et al., 2013). The western margin of the YC is bordered by the Pinjarra Orogen (PJO), which is largely covered by the Perth Basin (Figure 1a). The PJO evolved since the Mesoproterozoic along the western margin of the YC (Ksienzyk et al., 2012), and tracks the breakup of western Rodinia at *c.* 750 Ma and the final amalgamation of Gondwana at *c.* 520 Ma (Collins, 2003). The Gulden Draak and Batavia Knoll offshore microcontinents (Figure 1a) were once part of the PJO (Williams, Whittaker, Granot, & Müller, 2013).

Statement of significance

Time constrained Lu–Hf measurements of detrital zircon record >3 Gyr of crustal evolution in SW Australia, implying repeated episodic mixing of juvenile and evolved sources, commencing with a c. 4,000–3,800 Ma protocrust. In tandem with geophysical evidence, a Hadean–Eoarchean crustal remnant is inferred in the deep basement of the Yilgarn Craton along its SW margin. A widespread increase in the extraction/preservation of protocrust is interpreted to have occurred during this interval globally.

3 | METHODS

Samples in this work were selected to represent the crustal growth of SW Australia. We integrate (a) detrital zircon of modern littoral and fluvial sediments on the Scott Coastal Plain (Figure 1a; Western Australia), which represent multicyclic sediments that are sourced from the local crystalline basement (PJO, AFO and YC; Dröllner, Barham, & Kirkland, 2022; Sircombe & Freeman, 1999), and (b) published detrital zircon data of the Perth Basin, Hillier Bay, Arid Basin and Barren Basin (meta)sediments, all of which have been recognized as significant archives of detrital minerals derived from the PJO, AFO and/or YC (Kirkland, Barham, & Danišík, 2020; Olierook et al., 2019; Spaggiari et al., 2015). Detrital zircon grains have been analysed for their U–Pb and Lu–Hf isotopic compositions using laser ablation split stream-inductively coupled plasma-mass spectrometry at the John de Laeter Centre, Curtin University. Detailed analytical procedures and references for literature data (Table S1) are provided in the Supporting Information S1. Sample locations (Table S2) and results of reference materials (Tables S4 and S6) are listed in the Supporting Information S2.

Hf model ages use a two-stage evolution referenced to either depleted mantle (DM; T^2_{DM}) or CHondritic Uniform Reservoir (CHUR; T^2_{CHUR}). Model age calculations were performed for concordant zircon analyses utilizing the R package "detzrcr" (github.com/magnuskristoffersen/detzrcr) and use the ^{176}Lu decay constant of Söderlund, Patchett, Vervoort, and Isachsen (2004), the CHUR composition

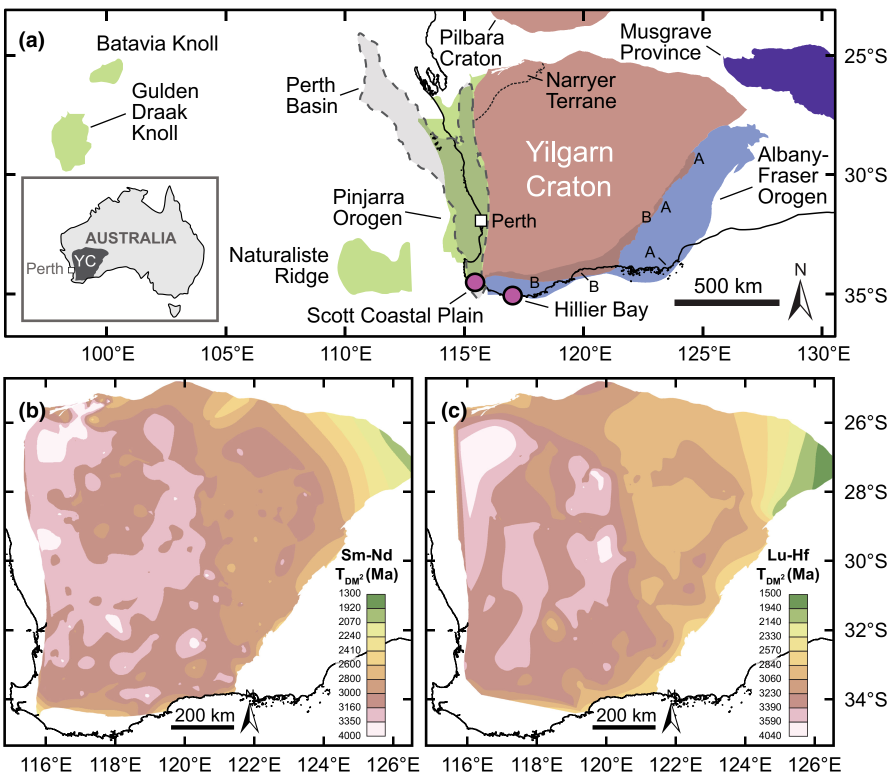

FIGURE 1 (a) Present-day locations of crustal units discussed in this work. Inset shows geographic extent of Yilgarn Craton (YC) within Australia, and "A" and "B" indicate major occurrences of the Arid and Barren basins respectively. (b) Spatially interpolated magmatic whole rock Sm–Nd and (c) zircon Lu–Hf two-stage depleted mantle model ages (T^2_{DM}) of the Yilgarn Craton. Isotopic data obtained from dmp.wa.gov.au/GeoView. [Colour figure can be viewed at wileyonlinelibrary.com]

of Bouvier, Vervoort, and Patchett (2008) and the DM values after Griffin et al. (2000). The latter are adjusted to the CHUR and decay constant values used herein. Model age calculations utilize a crustal $^{176}Lu/^{177}Hf$ ratio of 0.013 that is estimated from linear regression (see discussion).

4 | RESULTS AND DISCUSSION

4.1 | Provenance

Based on U–Pb geochronology (Figure 2; Table S3) and Lu–Hf isotope geochemistry (Figure 3a,b; Table S5), Scott Coastal Plain detrital zircon grains were sourced from local crystalline basement including the YC (*c*. 2,710–2,580 Ma), the AFO (*c*. 1,700–1,600 Ma and 1,240–1,120 Ma) and the PJO (*c*. 1,100–880 Ma and 730–500 Ma), or their equivalent pre-breakup terranes in Antarctica and India. The zircon Hf isotope data show low similarity to the Musgrave signature (Figure 3a) and suggest no significant derivation from central Australian lithologies. The source-to-sink correlation of the Scott Coastal Plain detritus to proximal sources is consistent with previous interpretations (Dröllner et al., 2022; Sircombe & Freeman, 1999).

4.2 | Crustal evolution

The Lu–Hf isotope geochemistry of detrital data (Figure 3b) broadly resembles that of zircon from regional crystalline basement rocks (Figure 3a). This suggests that the detrital data can be used as a proxy of regional crustal evolution, and provide a more complete record where inadequate preservation or exposure of the crystalline basement restricts direct crustal sampling. Most detrital zircon have sub-chondritic $\varepsilon Hf_{(t)}$ indicating crystallization from melts with crustal contamination. The three pronounced vertical arrays, at *c*. 2,700, 1,200 and 500 Ma, suggest mingling and mixing of evolved crustal and juvenile mantle-like sources (Figure 3b; Vervoort & Kemp, 2016).

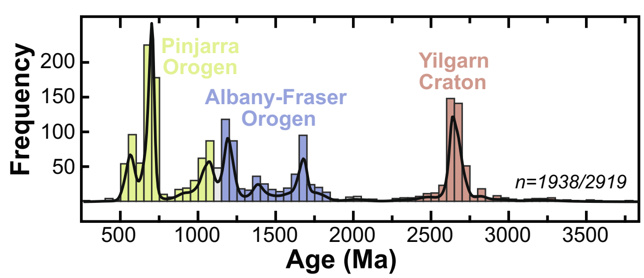

FIGURE 2 Kernel density estimates of U–Pb ages of detrital zircon from this study, Perth Basin (Olierook et al., 2019 and references therein), Hillier Bay (Kirkland et al., 2020) and AFO metasediments (Arid and Barren Basin; Spaggiari et al., 2015). *n* = number of analyses (concordant/total). [Colour figure can be viewed at wileyonlinelibrary.com]

The crustal units with ages that correspond to Hf-isotopic mixing arrays (2,700 Ma YC, 1,200 Ma AFO and 500 Ma PJO), all evolved in spatial proximity. Therefore, these indicative trends, that are best explained by mixing and are distinct from ancient Pb-loss trends (Figure 3b), are interpreted as a coherent ancient source terrane located at the juncture of these crustal units in SW Australia. The lower bound of the mixing arrays defines a continuous evolution trend towards an apparent Hadean–Eoarchean extraction (pink bar in Figure 3b). The slope of this evolution trend is consistent with a linear regression of the upper 1% of T^2_{DM} of the detrital record of SW Australia (Figure 3b). The slope of the evolution trend, based on the linear regression, corresponds to a $^{176}Lu/^{177}Hf$ ratio of 0.013 ± 1 (2σ). Using a larger proportion of the data, for example, the upper 2 or 5%, results in slopes within the uncertainty of the regression of the upper 1%. Hence, the proposed $^{176}Lu/^{177}Hf$ ratio of 0.013 is considered meaningful to extract compositional constraints on the ancient source terrane be they mixed or reflecting single reworked components.

The granite-greenstone YC shows a bimodal composition with SiO_2 modes at *c*. 50 and 73 wt% corresponding to $^{176}Lu/^{177}Hf$ of 0.029 and 0.005 respectively (Figure 4a). A $^{176}Lu/^{177}Hf$ ratio of 0.013 suggests crust with 59 wt% SiO_2 and approximates the average value for the YC based on lithological abundance and concentration (Figure 4a). However, a 0.013 $^{176}Lu/^{177}Hf$ value falls outside the YC compositional modes (Figure 4a), that is, this value neither corresponds to felsic nor mafic sources. This could imply that the apparent $^{176}Lu/^{177}Hf$ slope (Figure 3b) reflects a mixed source, petrologically analogous to the bulk average of Archean granite-greenstone crust. Based on binary mixing of felsic and mafic reservoirs (Table S7), a $^{176}Lu/^{177}Hf$ ratio of 0.013 is more mafic than the average exposed YC or Pilbara Craton (Figure 4b), but comparable to the lower Warrawoona Group of the Pilbara Craton (Figure 4a). Significantly, the 3,530–3,420 Ma Warrawoona Group, which is a volcano-sedimentary succession of mainly tholeiitic and komatiitic basalts, has been considered a compositional analogue of early Earth protocrust (Smithies, Champion, & van Kranendonk, 2009).

Using a $^{176}Lu/^{177}Hf$ ratio of 0.013, maximum T^2_{DM} ages are around 4,000 Ma and T^2_{CHUR} are around 3,800 Ma (Table S5). This evolutionary trend is best considered to represent a mixed source, given it does not correspond to a compositional mode in most Archean crust. Nonetheless, model ages derived from it provided a minimum constraint for the oldest component in that mixture. The proposed evolution array resembles the lower bound of time-integrated Hf evolution arrays of other areas hosting Archean crust globally (defined using the upper 1% of T^2_{DM}; Figure 3c). These trends also suggest unradiogenic crustal reservoirs that were episodically subjected to phases of crustal reworking with widespread protocrust formation at or before *c*. 4,000–3,800 Ma.

The global consistency of this isotopic legacy, capable of resisting dilution by repeated interaction with juvenile melts, likely requires a significant volume of protocrust. However, frequencies of model ages are likely altered by mixing processes that blur the temporal

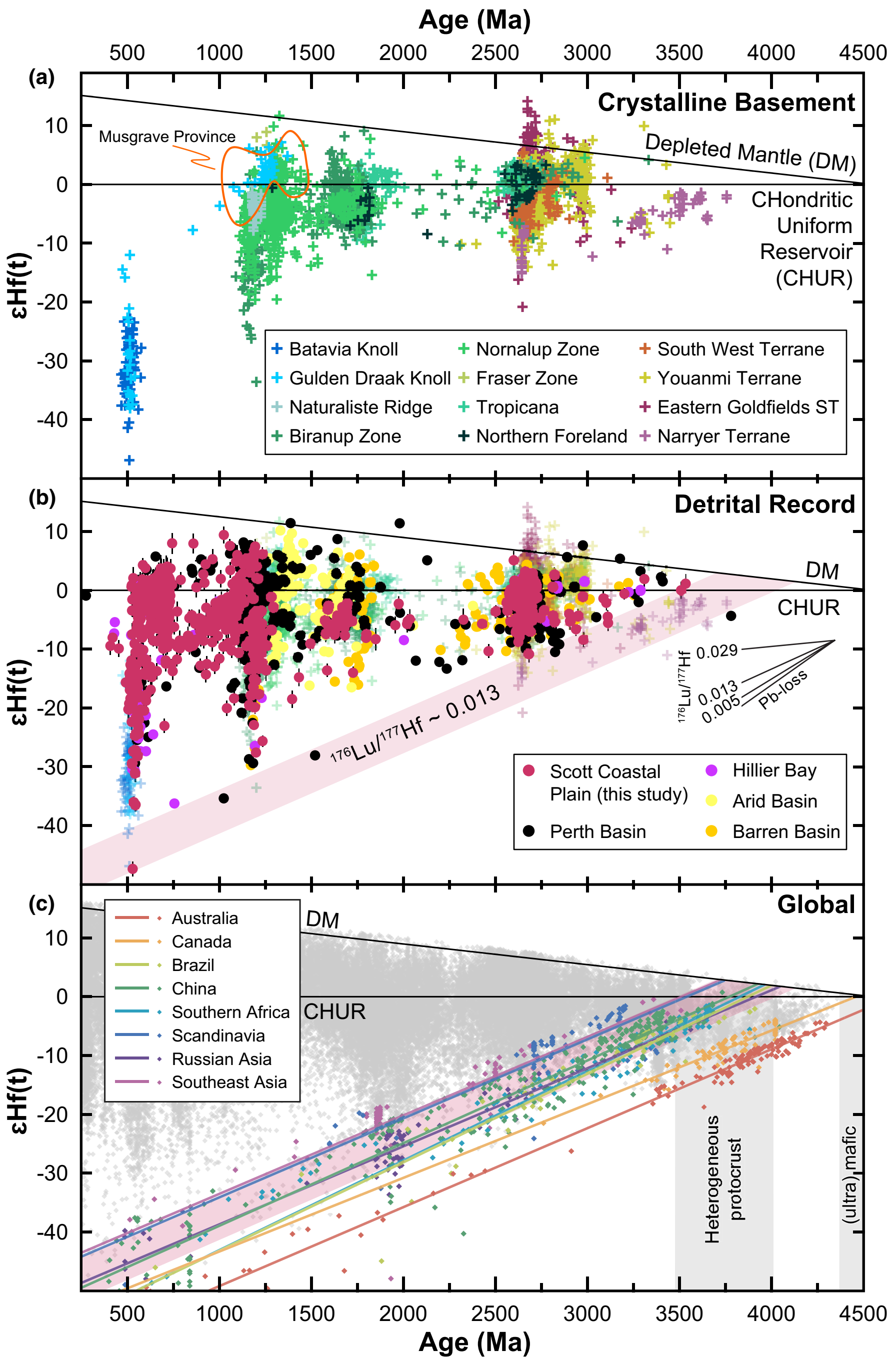

FIGURE 3 (a) Lu–Hf evolution plot of the crystalline basement of SW Australia and conjugate terranes (ST – Superterrane) [References for literature data are provided in Table S1 in the Supporting Information S1]. (b) Lu–Hf evolution plot of detrital zircon in SW Australia [References for literature data are provided in Figure 2]; pink array visualizes temporal evolution of the proposed Yilgarn protocrust; inset shows expected evolution trajectories for Pb-loss and different $^{176}Lu/^{177}Hf$ ratios. (c) Lu–Hf evolution plot of the global compilation (Puetz & Condie, 2019) of areas hosting Archean crust. Coloured data points are used for linear regression. Grey vertical bars show time frame of termination of Hf trends indicative of protocrust mantle extraction. [Colour figure can be viewed at wileyonlinelibrary.com]

resolution of the primary extraction (Figure 4c,d). Despite this, a high rate of change in global Hf model ages at 4,000–3,800 Ma (T^2_{DM} and T^2_{CHUR}, Figure 4c,d) implies an increase in protocrust formation consistent with a fundamental planetary geodynamic change point at this time (Figure 3b,c). This globally distinct change is less likely purely a relic of steady state preservation bias (e.g. Hawkesworth, Cawood, Kemp, Storey, & Dhuime, 2009), which would be expected to have resulted in a more gradual change. Regardless of it being due to formational or preservational drivers, the rate change identified indicates a shift in large scale crustal processes (whether tectonic or compositional) associated with ancient crust at this time. In addition, homogeneity tests suggest a change in crust production/preservation rates after *c.* 3,700 Ma (Pettitt's test; Figure 4c,d).

Significant volumes of pre-existing ancient crust are consistent with isotopic evidence for incorporation of ancient material in other parts of the YC (Mole et al., 2019; Morris & Kirkland, 2014), and support interpretations of early Earth fractionation processes (e.g. Bennett, Brandon, & Nutman, 2007). The similarity between CHUR and DM reservoirs on the early Earth results in a comparatively small difference between calculated model age modes using either model, with little implication for the timing of a broad secular change to Earth geodynamics (Figure 4c,d). Likewise, only

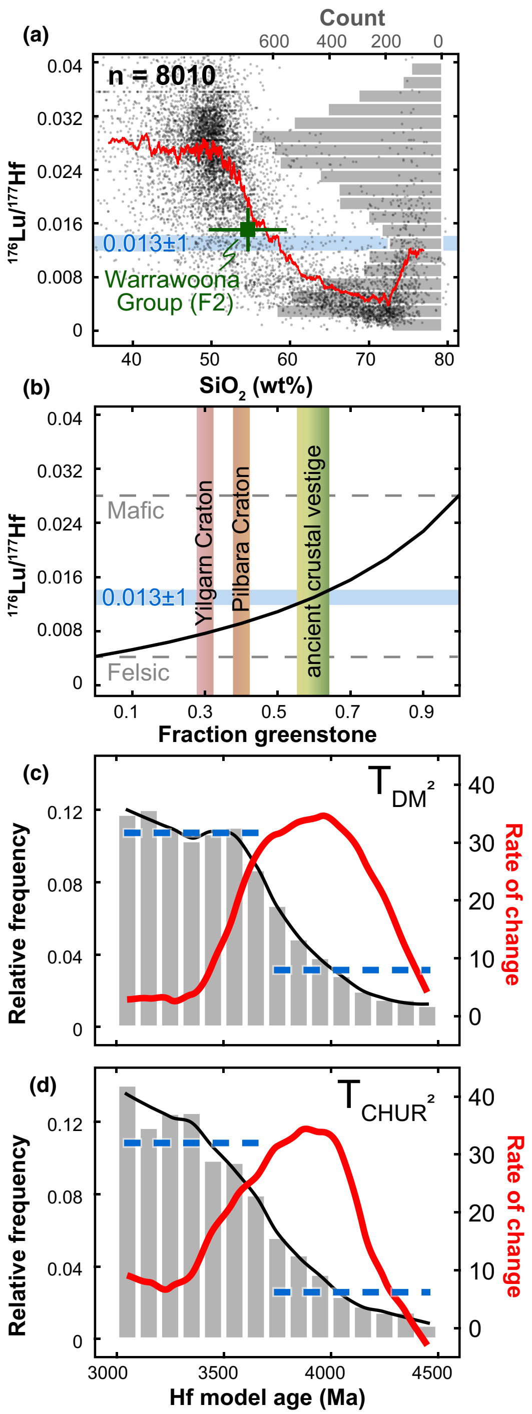

FIGURE 4 (a) ^{176}Lu/^{177}Hf ratio of (meta)igneous rocks of the YC calculated using whole rock geochemistry obtained from dmp.wa.gov.au/GeoView. Red and blue lines show running average and the ^{176}Lu/^{177}Hf value employed for model age calculations respectively. Green square indicates average composition of F2 sections of the Warrawoona group (Smithies et al., 2009). (b) Binary mixing model of end-members of Figure 4a, that is, a felsic and a mafic component with ^{176}Lu/^{177}Hf values of 0.029 and 0.005 respectively. Intercept of mixing model and ^{176}Lu/^{177}Hf of proposed evolution array of ancient crustal vestige indicates greenstone fraction. Fraction of greenstone for YC and Pilbara Craton is based on present-day extent (dmp.wa.gov.au/GeoView). (c) Relative frequency of T^2_{DM} and (d) T^2_{CHUR} Hf model ages of the global compilation (Puetz & Condie, 2019). Black and red lines show locally estimated scatterplot smoothing of the relative frequency and the rate of change (of the relative frequency) respectively. Blue-dashed lines indicate a homogeneity test (Pettitt's test) that reveals relative frequencies of T^2_{DM} and T^2_{CHUR} change at *c.* 3,700 Ma, rejecting the null hypothesis that the data are homogeneous at >99% confidence level. [Colour figure can be viewed at wileyonlinelibrary.com]

end-member scenarios of crustal ^{176}Lu/^{177}Hf ratios (Figure 4a) alter model results significantly, for example, a ^{176}Lu/^{177}Hf of 0.005 equates to a maximum T^2_{DM} of *c.* 3,700 Ma. However, modest variations consistent with the uncertainty of the regression (i.e. ±0.001), do not meaningfully change the dominant time of apparent crust extraction.

The trends of the most evolved zircon grains in Australia and Canada (Figure 3c) that are dictated by zircons from Jack Hills and Acasta, respectively, appear distinct to the broad *c.* 4,000–3,800 Ma source pattern seen globally (Figure 3c) suggesting earlier protocrust formation soon after planetary accretion, which is consistent with various distinct early geodynamic states (e.g. Drabon et al., 2022; Smithies et al., 2021). The significant offset from other evolution trends towards higher ^{176}Lu/^{177}Hf (Figure 3c) is most likely a reflection of different formation mechanisms for these two zircon populations, perhaps via some direct or indirect impact melt origin (e.g. Johnson et al., 2018). Such an observation implies no genetic relationship in the geodynamic environment between the Hadean protocrust of Jack Hills and Acasta, and the Yilgarn protocrust.

4.3 | An ancient vestige of protocrust hidden beneath the Yilgarn Craton

Gravity data (Figure 5a) suggest that the crust of the SW YC is significantly thicker and denser than that in the eastern terranes of the craton (Aitken, Salmon, & Kennett, 2013). A similar dense gravity response is identified in the Narryer Terrane and in an apparent interconnected western edge of the YC that stretches some 1,000 km southwards (Figure 5a; grey dashes). This geophysically anomalous area is coincident with older model ages of magmatic rock (Figure 5b). Reading, Kennett, and Dentith (2003) used seismic refraction data to identify a high-velocity zone in the lower crust of this area (Figure 5c), which we interpret as a deep remnant of a Yilgarn protocrust stretching north to the Narryer Terrane. Its eastern boundary trends north-west and aligns with several iron ore and gold deposits (e.g. Katanning, Karara), consistent with mineralization associated with a deep-seated crustal boundary (Outhwaite, 2018). Including the Narryer Terrane, a minimum extent of *c.* 100,000 km^2 can be inferred for this protocrust. Such a large volume of differentiated crust would have been associated with enhanced buoyancy (e.g. Santosh, Maruyama, & Yamamoto, 2009), a factor that likely

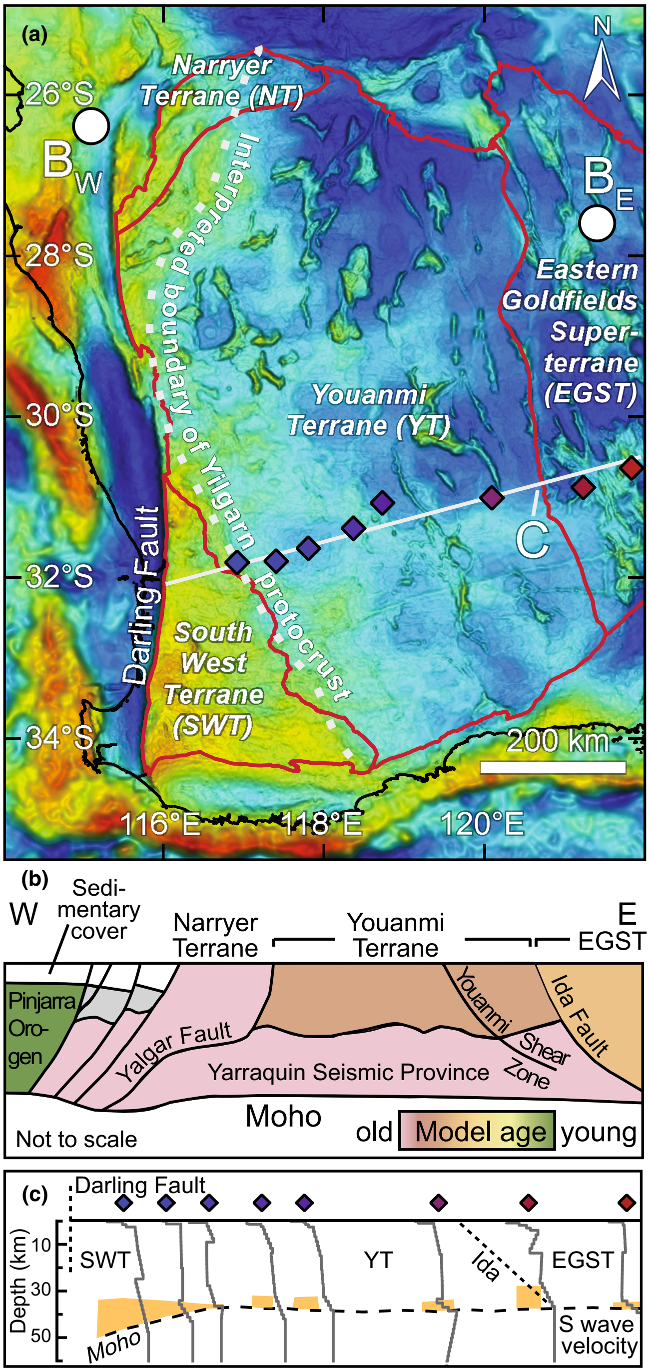

FIGURE 5 (a) Spherical Cap Bouguer gravity anomalies obtained from dmp.wa.gov.au/GeoView; blue to red colours correspond with low to high values. Grey dashes indicate interpreted boundary of Yilgarn protocrust. B_W and B_E are approximate endpoints of (b) showing a schematic cross-section of YC after Korsch et al. (2013); colour coding based on Sm–Nd T^2_{DM} (Figure 1b); model age interpretation of Yarraquin Seismic Province after Morris and Kirkland (2014). (c) Seismic interpretation of YC cross section (line C Figure 5a) after Reading et al. (2003); diamonds show receiver positions (Figure 5a); grey lines are best-fitting models; Moho is the base of the high-velocity gradient zones (orange). [Colour figure can be viewed at wileyonlinelibrary.com]

controlled its preservation and allowed the craton to grow, as recorded eastwards. The large volume could also imply coalescence of individual crustal seeds.

5 | CONCLUSIONS

U–Pb and Lu–Hf analyses of detrital zircon indicate the existence of an ancient crustal substrate beneath the SW of the Archean YC. This substrate is interpreted to be a remnant of Hadean–Eoarchean protocrust residing at depth outside the Narryer Terrane and compositionally similar to Archean granite-greenstone crust. This protocrust was subject to major episodes of later magmatic reworking over some 2 Gyr, as evidenced by at least three excursions towards more radiogenic average $\varepsilon Hf_{(t)}$ values. The persistence of this cryptic terrane is supported by geophysical measures that define a large block of distinct crust on the western edge of the YC. The global zircon Hf isotope record also highlights an apparent *c.* 4,000–3,800 Ma period of extensive crust formation, which contrasts with isotopic records from Acasta and Jack Hills that likely reflect a distinct, earlier, geodynamic state. Extensive protocrust formation at 4,000–3,800 Ma appears to have provided crustal seeds that supported episodic continental growth well-beyond the Archean.

ACKNOWLEDGEMENTS

This research was supported by the Minerals Research Institute of Western Australia grant M551. We thank Rohan Hine and David Sleigh of Iluka Resources for samples, Elizabeth Bell and Martin Guitreau for constructive comments that have improved this work significantly, and Klaus Mezger for editorial handling. GeoHistory Facility (JdLC) is supported by AuScope (auscope.org.au), the NCRIS, and the LIEF program (LE150100013). Open access is made available through the Read & Publish agreement of Wiley and the Council of Australian University Librarians.

DATA AVAILABILITY STATEMENT

The data that support the findings of this study are available in the supporting information of this article.

ORCID

Maximilian Dröllner https://orcid.org/0000-0001-8661-9565
Christopher L. Kirkland https://orcid.org/0000-0003-3367-8961
Milo Barham https://orcid.org/0000-0003-0392-7306
Noreen J. Evans https://orcid.org/0000-0002-7615-8328

REFERENCES

Aitken, A., Salmon, M. L., & Kennett, B. (2013). Australia's Moho: A test of the usefulness of gravity modelling for the determination of Moho depth. *Tectonophysics*, *609*, 468–479.

Bennett, V. C., Brandon, A. D., & Nutman, A. P. (2007). Coupled ^{142}Nd-^{143}Nd isotopic evidence for hadean mantle dynamics. *Science*, *318*, 1907–1910.

Bouvier, A., Vervoort, J. D., & Patchett, P. J. (2008). The Lu–Hf and Sm–Nd isotopic composition of CHUR: Constraints from unequilibrated chondrites and implications for the bulk composition of terrestrial planets. *Earth and Planetary Science Letters*, *273*, 48–57.

Cassidy, K. F., Champion, D. C., Krapez, B., Barley, M. E., Brown, S. J., Blewett, R. S., … Tyler, I. M. (2006). *A revised geological framework for the Yilgarn craton, Western Australia, Record 2006/8*. Geological Survey of Western Australia.

Collins, A. S. (2003). Structure and age of the northern Leeuwin complex, Western Australia: Constraints from field mapping and U–Pb isotopic analysis. *Australian Journal of Earth Sciences*, *50*, 585–599.

Drabon, N., Byerly, B. L., Byerly, G. R., Wooden, J. L., Wiedenbeck, M., Valley, J. W., Kitajima, K., Bauer, A. M., & Lowe, D. R. (2022). Destabilization of long-lived hadean Protocrust and the onset of pervasive hydrous melting at 3.8 Ga. *AGU Advances*, *3*, e2021AV000520.

Dröllner, M., Barham, M., & Kirkland, C. L. (2022). Gaining from loss: Detrital zircon source-normalized α-dose discriminates first- versus multi-cycle grain histories. *Earth and Planetary Science Letters*, *579*, 117346.

Goodwin, A. M. (1996). *Principles of precambrian geology*. Academic Press.

Griffin, W. L., Belousova, E. A., Shee, S. R., Pearson, N. J., & O'Reilly, S. Y. (2004). Archean crustal evolution in the northern Yilgarn Craton: U–Pb and Hf-isotope evidence from detrital zircons. *Precambrian Research*, *131*, 231–282.

Griffin, W. L., Pearson, N. J., Belousova, E., Jackson, S. E., van Achterbergh, E., O'Reilly, S. Y., & Shee, S. R. (2000). The Hf isotope composition of cratonic mantle: LAM-MC-ICPMS analysis of zircon megacrysts in kimberlites. *Geochimica et Cosmochimica Acta*, *64*, 133–147.

Guitreau, M., Boyet, M., Paquette, J.-L., Gannoun, A., Konc, Z., Benbakkar, M., Suchorski, K., & Hénot, J.-M. (2019). Hadean protocrust reworking at the origin of the Archean Napier complex (Antarctica). *Geochemical Perspectives Letters*, *12*, 7–11.

Hawkesworth, C., Cawood, P., Kemp, T., Storey, C., & Dhuime, B. (2009). A matter of preservation. *Science*, *323*, 49–50.

Johnson, T. E., Gardiner, N. J., Miljković, K., Spencer, C. J., Kirkland, C. L., Bland, P. A., & Smithies, H. (2018). An impact melt origin for Earth's oldest known evolved rocks. *Nature Geoscience*, *11*, 795–799.

Kinny, P. D., Williams, I. S., Froude, D. O., Ireland, T. R., & Compston, W. (1988). Early Archaean zircon ages from orthogneisses and anorthosites at mount Narryer, Western Australia. *Precambrian Research*, *38*, 325–341.

Kirkland, C. L., Barham, M., & Danišík, M. (2020). Find a match with triple-dating: Antarctic sub-ice zircon detritus on the modern shore of Western Australia. *Earth and Planetary Science Letters*, *531*, 115953.

Kirkland, C. L., Smithies, R. H., Woodhouse, A. J., Howard, H. M., Wingate, M. T., Belousova, E. A., Cliff, J. B., Murphy, R. C., & Spaggiari, C. V. (2013). Constraints and deception in the isotopic record; the crustal evolution of the west Musgrave Province, Central Australia. *Gondwana Research*, *23*, 759–781.

Kirkland, C. L., Spaggiari, C. V., Pawley, M. J., Wingate, M., Smithies, R. H., Howard, H. M., Tyler, I. M., Belousova, E. A., & Poujol, M. (2011). On the edge: U–Pb, Lu–Hf, and Sm–Nd data suggests reworking of the Yilgarn craton margin during formation of the Albany-Fraser orogen. *Precambrian Research*, *187*, 223–247.

Korsch, R. J., Blewett, R. S., Johnson, S. P., van Kranendonk, M. J., Patison, N., Kennett, B., Jones, T., et al. (2013). *Geodynamic implications of the Youanmi and southern Carnarvon deep seismic reflection surveys: A ~1300 km traverse from the Pinjarra orogen to the eastern Yilgarn craton: Record 2013/6*. Geological Survey of Western Australia.

Ksienzyk, A. K., Jacobs, J., Boger, S. D., Košler, J., Sircombe, K. N., & Whitehouse, M. J. (2012). U–Pb ages of metamorphic monazite and detrital zircon from the Northampton complex: Evidence of two orogenic cycles in Western Australia. *Precambrian Research*, *198-199*, 37–50.

Mole, D. R., Kirkland, C. L., Fiorentini, M. L., Barnes, S. J., Cassidy, K. F., Isaac, C., Belousova, E. A., Hartnady, M., & Thebaud, N. (2019). Time-space evolution of an Archean craton: A Hf-isotope window into continent formation. *Earth-Science Reviews*, *196*, 102831.

Morris, P. A., & Kirkland, C. L. (2014). Melting of a subduction-modified mantle source: A case study from the Archean Marda volcanic complex, central Yilgarn craton, Western Australia. *Lithos*, *190-191*, 403–419.

Olierook, H. K., Barham, M., Fitzsimons, I. C., Timms, N. E., Jiang, Q., Evans, N. J., & McDonald, B. J. (2019). Tectonic controls on sediment provenance evolution in rift basins: Detrital zircon U–Pb and Hf isotope analysis from the Perth Basin, Western Australia. *Gondwana Research*, *66*, 126–142.

Outhwaite, M. D. (2018). *Metamorphosed Mesoarchean cu-Mo-ag mineralization: Evidence from the Calingiri deposits, southwest Yilgarn craton, report 183*. Geological Survey of Western Australia.

Petersson, A., Kemp, A. I., & Whitehouse, M. J. (2019). A Yilgarn seed to the Pilbara craton (Australia)? Evidence from inherited zircons. *Geology*, *47*, 1098–1102.

Puetz, S. J., & Condie, K. C. (2019). Time series analysis of mantle cycles part I: Periodicities and correlations among seven global isotopic databases. *Geoscience Frontiers*, *10*, 1305–1326.

Reading, A. M., Kennett, B. L. N., & Dentith, M. C. (2003). Seismic structure of the Yilgarn craton, Western Australia. *Australian Journal of Earth Sciences*, *50*, 427–438.

Santosh, M., Maruyama, S., & Yamamoto, S. (2009). The making and breaking of supercontinents: Some speculations based on superplumes, super downwelling and the role of tectosphere. *Gondwana Research*, *15*, 324–341.

Sircombe, K. N., & Freeman, M. J. (1999). Provenance of detrital zircons on the Western Australia coastline—Implications for the geologic history of the Perth basin and denudation of the Yilgarn craton. *Geology*, *27*, 879–882.

Smithies, R. H., Lu, Y., Kirkland, C. L., Johnson, T. E., Mole, D. R., Champion, D. C., Martin, L., Jeon, H., Wingate, M. T. D., & Johnson, S. P. (2021). Oxygen isotopes trace the origins of Earth's earliest continental crust. *Nature*, *592*, 70–75.

Smithies, R. H., Champion, D. C., & van Kranendonk, M. J. (2009). Formation of Paleoarchean continental crust through infracrustal melting of enriched basalt. *Earth and Planetary Science Letters*, *281*, 298–306.

Söderlund, U., Patchett, P., Vervoort, J. D., & Isachsen, C. E. (2004). The ^{176}Lu decay constant determined by Lu–Hf and U–Pb isotope systematics of Precambrian mafic intrusions. *Earth and Planetary Science Letters*, *219*, 311–324.

Spaggiari, C. V., Kirkland, C. L., Smithies, R. H., Wingate, M., & Belousova, E. A. (2015). Transformation of an Archean craton margin during Proterozoic basin formation and magmatism: The Albany–Fraser orogen, Western Australia. *Precambrian Research*, *266*, 440–466.

Vervoort, J. D., & Kemp, A. I. (2016). Clarifying the zircon Hf isotope record of crust–mantle evolution. *Chemical Geology*, *425*, 65–75.

Wilde, S. A., Valley, J. W., Peck, W. H., & Graham, C. M. (2001). Evidence from detrital zircons for the existence of continental crust and oceans on the earth 4.4 Gyr ago. *Nature*, *409*, 175–178.

Williams, S. E., Whittaker, J. M., Granot, R., & Müller, D. R. (2013). Early India-Australia spreading history revealed by newly detected Mesozoic magnetic anomalies in the Perth abyssal plain. *Journal of Geophysical Research: Solid Earth*, *118*, 3275–3284.

Wyche, S., Nelson, D. R., & Riganti, A. (2004). 4350–3130 Ma detrital zircons in the southern cross granite-greenstone terrane, Western Australia: Implications for the early evolution of the Yilgarn craton. *Australian Journal of Earth Sciences*, *51*, 31–45.

SUPPORTING INFORMATION

Additional supporting information can be found online in the Supporting Information section at the end of this article.

Appendix S1

Appendix S2

How to cite this article: Dröllner, M., Kirkland, C. L., Barham, M., Evans, N. J., & McDonald, B. J. (2022). A persistent Hadean–Eoarchean protocrust in the western Yilgarn Craton, Western Australia. *Terra Nova*, *34*, 458–464. https://doi.org/10.1111/ter.12610